

Di(2-pyridyl)-Amides and -Phosphides: Syntheses, Reactivity, Structures, Raman-Experiments and Calculations

Matthias Pfeiffer¹, Frank Baier¹, Thomas Stey¹, Dirk Leusser¹, Dietmar Stalke¹, Bernd Engels², Damien Moigno³, and Wolfgang Kiefer³

¹Institut für Anorganische Chemie der Universität Würzburg, Am Hubland, D-97074 Würzburg, Germany. Tel.: +49-931-888-4783; Fax: +49-931-888-4619. E-mail: dstalke@chemie.uni-wuerzburg.de

²Institut für Organische Chemie der Universität Würzburg, Am Hubland, D-97074 Würzburg, Germany

³Institut für Physikalische Chemie der Universität Würzburg, Am Hubland, D-97074 Würzburg, Germany

Received: 1 October 1999/ Accepted: 25 January 2000/ Published: 28 February 2000

Abstract The 2-pyridyl containing compounds (2-Py)₂NH **1**, (2-Py)₂PH **2**, Me₂Al(2-Py)₂N **3**, Me₂Al(2-Py)₂P **4**, Et₂Al(2-Py)₂N **5**, Et₂Al(2-Py)₂P **6** and Et₂Al(2-Py)₂NAI Et₃ **7** have been synthesized and analyzed by solid state structure determination, FT-Raman spectroscopy and theoretical calculations in order to elucidate the charge density distribution. All di(2-pyridyl) amides and -phosphides coordinate the R₂Al⁺ fragment *via* both ring nitrogen atoms, but the Lewis basicity of the central two-coordinated nitrogen atom in **5** is high enough to coordinate a second equivalent AlEt₃ to form the Lewis acid base adduct Et₂Al(2-Py)₂NAI Et₃ **7**. Several density functionals (BLYP, B3LYP, BPW91) have been examined in relation to various basis sets (6-31G, 6-31+G, 6-31G(d), 6-31+G(d)). This computational tool facilitates the unambiguous assignment of the Raman ring vibration frequencies. The shift to higher wavenumbers proceeding from the parent di(2-pyridyl)amine **1** and di(2-pyridyl)-phosphane **2** to the metal complexes **3** and **4** indicates partial double bond localization in the ring positions 3 and 5. This effect is more pronounced in the di(2-pyridyl)amide complexes than in the phosphide. Due to the higher electronegativity of the central nitrogen atom in **3**, **5** and **7** compared to the bridging two-coordinated phosphorus atom in **4** and **6** the di(2-pyridyl)amide is the harder Lewis base. In the phosphides nearly all charge density couples into the rings leaving the central phosphorus atom only attractive for soft metals.

Keywords Aluminum, Pyridyl-ligands, Amides, Phosphides, IR/Raman spectroscopy, DFT

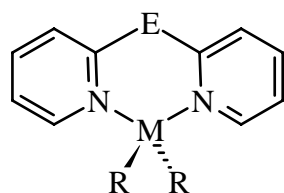
Correspondence to: D. Stalke

Dedicated to Professor Paul von Ragué Schleyer, the protagonist of applied computational chemistry and a true scholar, on the occasion of his 70th birthday

Introduction

N-Heteroaryl ring systems are well-known as bridging functions between transition metal centers.[1] Recently we described related complexes of di(2-pyridyl)amides, -phosphides and -arsenides Py₂E⁻ (E = N, P, As) with main group

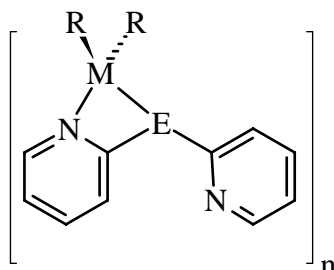
Scheme 1 Complexes of di(2-pyridyl)amides, -phosphides and -arsenides



E = N, P, As

M = Li; R = thf **A**

M = Al, Ga; R = Me



E = N, R = Me

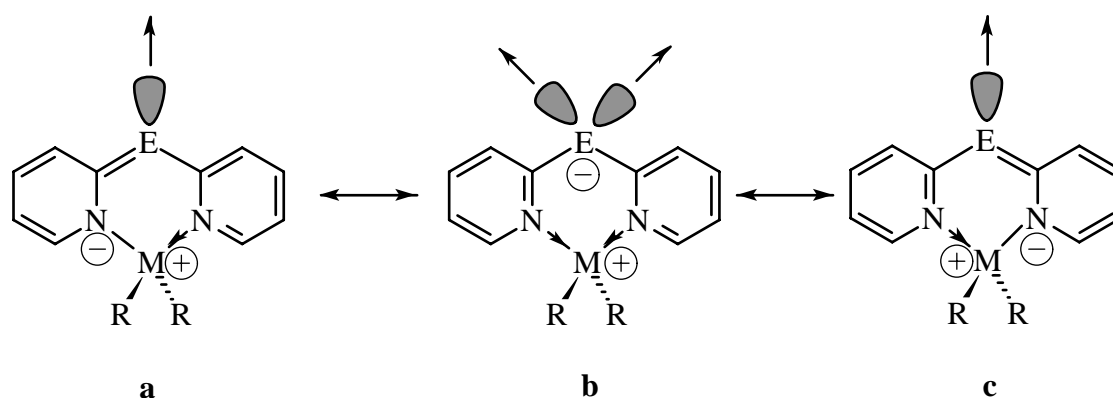
M = In, n = 2 **B**

M = Tl, n = ∞

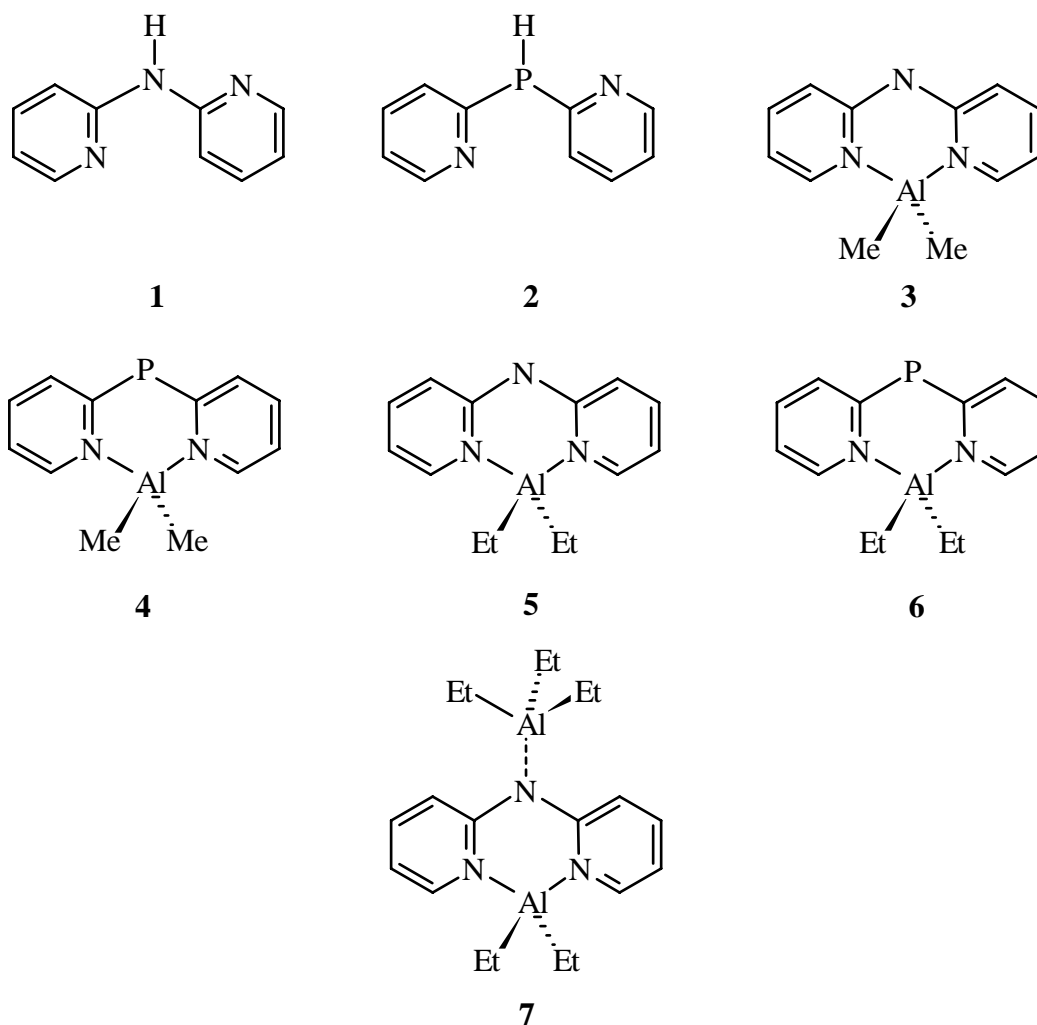
metal fragments, mainly group 13 metal organics.[2-4] The resulting low molecular aggregates contain group 13 and 15 elements and are of interest as volatile precursors for III/V semiconducting films.[5] The main feature of the ligands is the flexible chelating coordination behavior towards the various metal centers. They either coordinate exclusively by both pyridyl nitrogen atoms leaving the bridging E atom two-coordinated without any metal contact (**A** in Scheme 1)[2-4,6] or in a mixed bridging-N/ring-N fashion in some di(2-pyridyl)amides and di(2-pyridyl)phosphides (**B** in Scheme 1).[3,7]

The two-coordinated bridging atom (N, P, As) in complexes described in **A** should in principle be able to coordinate either one or even two further Lewis acidic metals. According to the mesomeric structures, it can act as a 2e⁻ or even a 4e⁻ donor. (Scheme 2)

In this paper we describe essential differences of these compounds concerning a further coordination of the bridging nitrogen or phosphorus atom from a synthetic, analytical (Raman spectroscopy) and theoretical (DFT calculations) point of view. Raman spectroscopy is an important additional tool in the determination of structural parameters of new compounds. The present class of compounds have not yet been studied conclusively by this method. Therefore we studied the vibrational behavior of the known compounds (2-Py)₂NH **1**[8], (2-Py)₂PH **2**[2], Me₂Al(2-Py)₂N **3**[3] and Me₂Al(2-Py)₂P **4**[2], and assigned vibrational modes with assistance of the results from density functional theory (DFT) calculations. These results explain why Et₂Al(2-Py)₂N **5** reacts with a second equivalent of Et₃Al to give the adduct Et₂Al(2-Py)₂NAIEt₃ **7** while the analogue phosphorus compound Et₂Al(2-Py)₂PAIEt₃ is not observed.



Scheme 2 Mesomeric structures of R₂M(2-Py)₂E



Scheme 3 Compounds described in this paper

Chemical results and discussion

Preparation of 5-7

Di(2-pyridyl)amine **1**[8] and di(2-pyridyl)phosphane **2**[2] were reacted with an equimolar amount of triethyl aluminum in Et_2O at -78°C leading to ethane and diethyl aluminum amide **5** and -phosphide **6**, respectively. The diethyl aluminum fragment is coordinated *via* both pyridyl N-atoms and the bridging atom N or P is left two-coordinated. Adding a second equivalent of triethyl aluminum to $\text{Et}_2\text{Al}(2\text{-Py})_2\text{N}$ **5** the adduct $\text{Et}_2\text{Al}(2\text{-Py})_2\text{NAlEt}_3$ **7** is formed where the bridging N-atom coordinates to the Lewis acid Et_3Al (Eq. (1) in scheme 4). Similar coordination features for the $(2\text{-Py})\text{N}^-$ ligand have been reported in the literature.[9] However, $\text{Et}_2\text{Al}(2\text{-Py})_2\text{P}$ **6**

does not form an adduct with a second equivalent of Et_3Al . Monitoring the reaction by ^{31}P -NMR there is no other signal raising than this from **6** at 23.7 ppm. In contrast to $\text{Et}_2\text{Al}(2\text{-Py})_2\text{N}$ **5**, the P atom in $\text{Et}_2\text{Al}(2\text{-Py})_2\text{P}$ **6** is not Lewis basic enough to coordinate to the hard Lewis acid Et_3Al (Eq (2) in scheme 4).

Crystal structure of 6

In the monomeric complex $\text{Et}_2\text{Al}(2\text{-Py})_2\text{P}$ **6** the aluminum and phosphorus atoms are μ_2 -bridged by two pyridyl ring systems (Figure 1). The phosphorus atom is two-coordinated and the two crystallographically independent P-C bonds are identical within estimated standard deviations (P1-C1 177.7(3); P1-C6 177.8(3) pm), indicating a delocalization of the negative charge throughout the anion. A P-C single bond

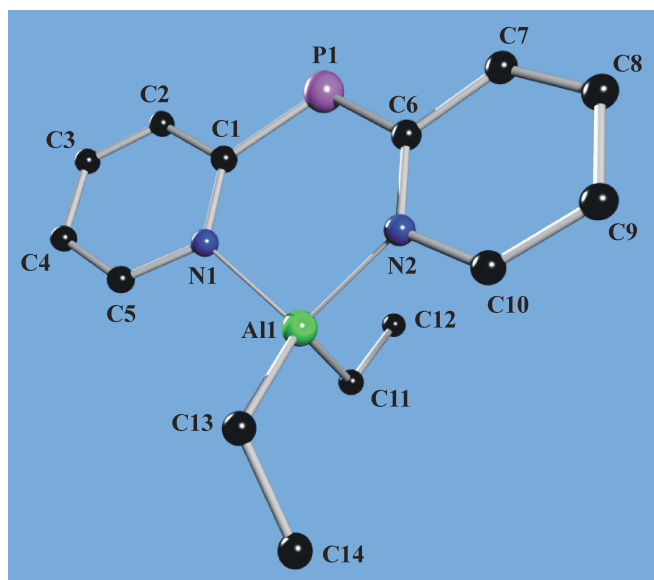
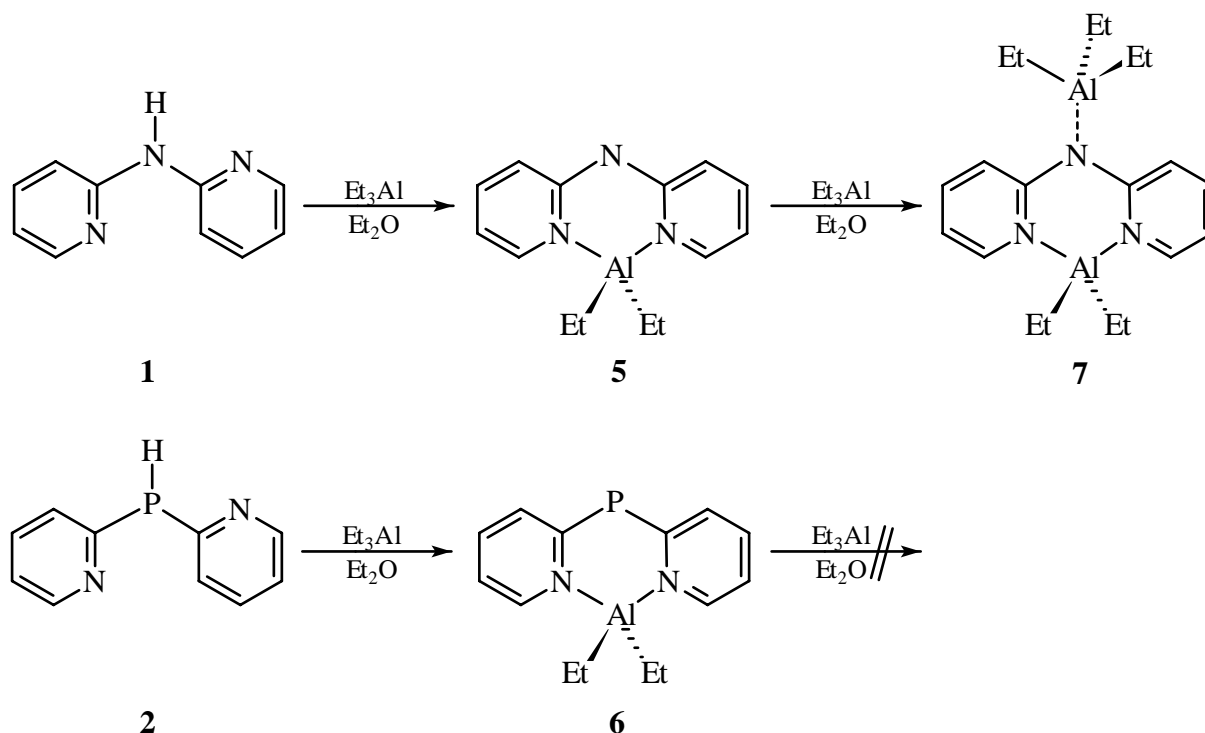


Figure 1 Molecular structure of $\text{Et}_2\text{Al}(2\text{-Py})_2\text{P}$ **6** in the solid state, selected bond lengths [pm] and angles [$^\circ$]; see also Tables 1 and 3: P1-C1 177.7(3), P1-C6 177.8(3), Al1-N1 192.4(2), Al1-N2 192.3(2), Al1-C11 196.4(3), Al1-C13 196.6(3), C1-P1-C6 107.40(13), P1-C1-N1 127.6(2), P1-C6-N2 127.3(2), C1-N1-Al1 124.3(2), C6-N2-Al1 125.2(2), N1-Al1-N2 100.04(10), C11-Al1-C13 118.04(13)

is about 185 pm long while the values for $\text{P}=\text{C}$ double bonds in phosphalkenes range from 161 to 171 pm.[10] Al1 shows a distorted tetrahedral coordination sphere. Both Al-N bonds are of the same length (192.4(2) and 192.3(2) pm) and correspond well to the related value in $\text{Me}_2\text{Al}(2\text{-Py})_2\text{N}$ **3** [3] (av. 192.4(2) pm). While the Al-N bond in the three-coordinated aluminum triamide $\text{Al}[\text{N}(\text{SiMe}_3)_2]_3$ [11] is 14 pm shorter than in **6**, the Al-N donor bond in $\text{P}(2\text{-Py})_3\text{AlMe}_3$ [2] is about 13 pm longer. Consequently, the Al-N bond in **6** ranges between a single bond and a donor bond. As in **4** and **6**, the P atom in $\text{Me}_2\text{Al}(\mu\text{-NMes}^*)_2\text{P}$ [12] is only two-coordinated. The Al-N distance in the AlN_2P ring system is 6 pm longer than in **4** and **6**. The Al-C bond lengths (av. 196.5 pm) are in accordance with those in related systems.[13]

The two pyridyl ring planes in **6** intersect at an angle of 163° . The related angle in $\text{Me}_2\text{Al}(2\text{-Py})_2\text{P}$ **4** is 155° in contrast to $(\text{thf})_2\text{Li}(2\text{-Py})_2\text{P}$,[2] where the deviation from planarity is only marginal (173°). Therefore the ethyl groups are nonequivalent in the solid state. Nevertheless, ^1H and ^{13}C spectra from solution show only one signal for the C atoms of the ethyl groups even at low temperature. The “bite” of the ligand (N...N distance) in such compounds ranges from 292.2 pm in **4**, 294.8 pm in **6** up to 306.4 pm in the nearly planar $(\text{thf})_2\text{Li}(2\text{-Py})_2\text{P}$, respectively. Hence the ligand shows coordination flexibility towards different metal fragments, while not giving up the full conjugation.



Scheme 4 Reactivity of $(2\text{-Py})_2\text{NH}$ and $(2\text{-Py})\text{P}_2\text{H}$

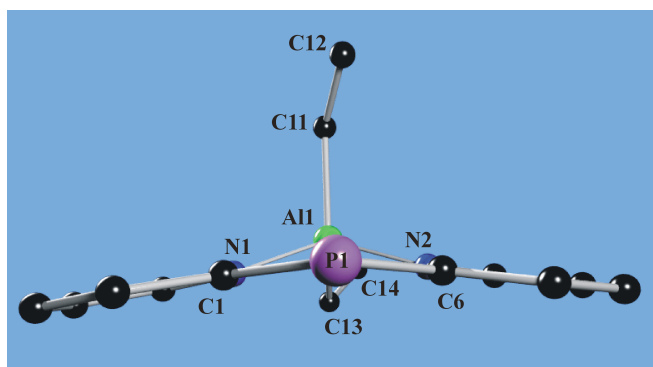


Figure 2 View along the P-Al axes of $\text{Et}_2\text{Al}(2\text{-Py})_2\text{P}$ **6** illustrating the butterfly conformation

Crystal structure of 7

In $\text{Et}_2\text{Al}(2\text{-Py})_2\text{NAlEt}_3$ **7** the coordination mode of the Et_2Al^+ fragment is similar to complex **6**. Al1 is coordinated by two pyridyl rings (Figure 3). The bridging N atom in contrast to the P atom in **6** is no longer two-coordinated. It forms a third bond to a second equivalent of the Lewis acid Et_3Al . The two N-C bond lengths are identical within estimated standard deviations (N2-C1 139.2(5) pm; N2-C6 138.3(4) pm), indicating a delocalization of the negative charge as in **6**, but the central N-C bonds in the adduct are considerably longer than in the parent $\text{Me}_2\text{Al}(2\text{-Py})_2\text{N}$ **3** (av. 134.3(2) pm). A N-C single bond is about 147 pm long while the bond length for a N=C double bond is about 129 pm.[14] Al1 and Al2 show a distorted tetrahedral coordination sphere. Both Al1-N bonds (193.3(3) and 191.1(4) pm) are of nearly the same length and similar to those in **3** (av. 191.5(2) pm), **4** (192.1(2) pm), and **6** (192.4(2) pm). Consequently, the Al1-N bonds in **7** range

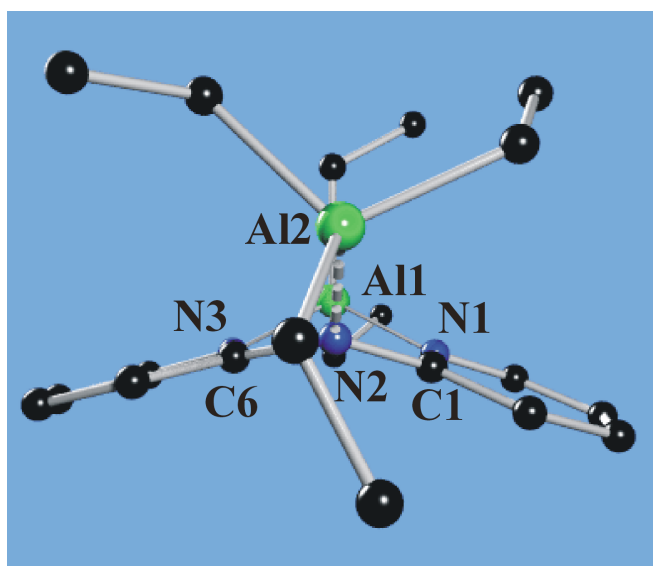


Figure 4 View along the N2-Al1 axes of $\text{Et}_2\text{Al}(2\text{-Py})_2\text{NAlEt}_3$ **7**

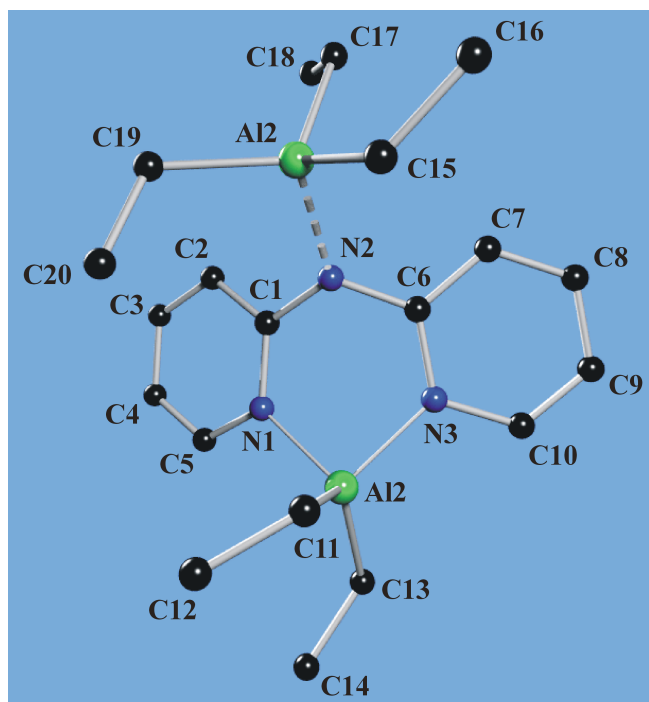


Figure 3 Molecular structure of $\text{Et}_2\text{Al}(2\text{-Py})_2\text{NAlEt}_3$ **7** in the solid state, selected bond lengths [pm] and angles [°]; see also Tables 1 and 3: N2-C1 139.2(5), N2-C6 138.3(4), N2-Al2 201.0(3), Al2-C15 199.5(4), Al2-C17 198.7(4), Al2-C19 198.1(4), Al1-N1 193.3(3), Al1-N3 191.1(4), Al1-C11 194.9(4), Al1-C13 195.4(4), C1-N2-C6 122.4(3), N2-C1-N1 122.1(3), N2-C6-N3 120.5(4), C1-N1-Al1 120.4(2), C6-N3-Al1 121.0(3), N1-Al1-N3 91.57(14), C11-Al1-C13 122.7(2), N2-Al2-C15 105.24(14), N2-Al2-C17 109.04(14), N2-Al2-C19 106.2(2)

between a single bond and a donor bond. Because of the formation of a donor bond to the Et_3Al -fragment in the adduct **7**, the bridging N atom is three-coordinated. The N2-Al2 bond of 201.0(3) pm is a typical Al-N donor bond.[2] Due to the Lewis acid base adduct formation, the N-C_{ipso} bonds are lengthened considerably to 138.8(4) pm in comparison to 134.3(2) pm in $\text{Me}_2\text{Al}(2\text{-Py})_2\text{N}$ **3**. While the Al1-C distances are marginally shorter (av. 195.2(4) pm) than the Al2-C distances (av. 198.8(4) pm), both values fit the range covered by organoaluminum compounds.[15]

It is worth noting that the two aluminum atoms in **7** are not located in the plane of the amide anion. As in the phosphide anion in **6** and in contrast to the planar complex $\text{Me}_2\text{Al}(2\text{-Py})_2\text{N}$ **3** it adopts a butterfly conformation. The planes of the two pyridyl rings intersect at an angle of 155.7°. Interestingly, the Al atom of the Et_3Al Lewis acid is located at the same side as the Et_2Al^+ aluminum atom. While the Al1 atom of the Et_2Al^+ moiety is 86.2 pm above the best plane of the three nitrogen atoms, the Al2 of the Et_3Al Lewis acid is 96.2 pm above that plane (Figure 4)

Although the ethyl groups are magnetically nonequivalent in the solid state, they equilibrate in the ^1H and ^{13}C spectra in

Table 1 Selected calculated and experimental structural parameters for $\text{Py}_2\text{NH 1}$ (bond lengths [pm], angles [$^\circ$])

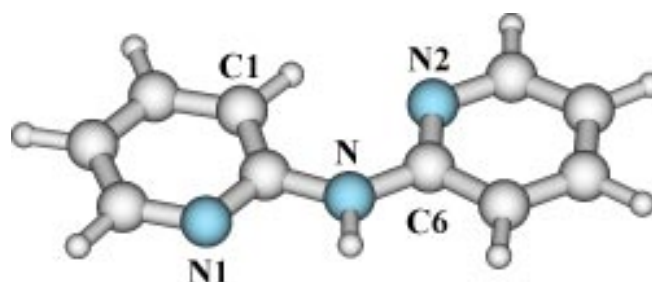
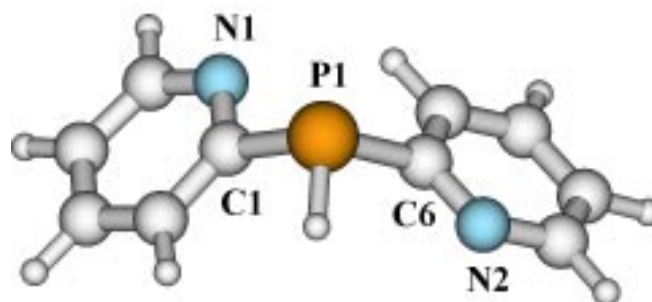
	B3LYP/ 6-31+G*	BPW91/ 6-31+G*	Expt. [a]
N1-H1	101.3	102.1	84.0(2)
N1-C1	139.0	139.4	138.7(2)
C1-N2	134.2	135.2	133.2(2)
N2-C5	133.9	134.6	133.9(2)
C5-C4	139.3	140.0	136.0(2)
C4-C3	140.0	140.6	137.3(3)
C3-C2	139.0	139.6	136.6(3)
C2-C1	141.2	141.8	139.0(2)
C1-N1-C6	132.5	132.7	131.0(2)

[a] values from [16c]; av. of four crystallographically independent pyridyl rings in the asymmetric unit; structure determination at 150 K

solution at room temperature. Even at low temperature it is not possible to verify the asymmetry and to freeze out different signals.

Experimental and computational structures

It is obvious from the experimental data of all $(2\text{-Py})_2\text{N}^-$ and $(2\text{-Py})_2\text{P}^-$ anions that significant shortening of the central N-C and P-C bonds occurs on going from the parent neutral amine $(2\text{-Py})_2\text{NH 1}$ to the amide and from the neutral phosphane $(2\text{-Py})_2\text{PH 2}$ to the phosphides. The pyridyl rings in the charged ligands exhibit alternating bond lengths, i. e. short bonds in the 3- and 5-positions, in contrast to the delocalized rings in **1** and **2**. With the amides their structures can be compared to experimental solid state crystal structure data of the amine $(2\text{-Py})_2\text{NH 1}$ [16], but such data for the phosphane $(2\text{-Py})_2\text{PH 2}$ are not available. Therefore, we decided to calculate and optimize the structures with density functional methods at a high level of theory. The B3LYP and BPW91 functionals gave the best results with the 6-31+G*

**Figure 5** BPW91/6-31+G* optimized geometry of $(2\text{-Py})_2\text{NH 1}$ **Figure 6** BPW91/6-31+G* optimized geometry of $(2\text{-Py})_2\text{PH 2}$

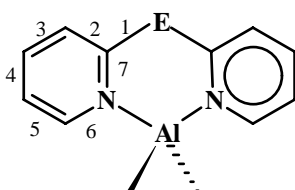
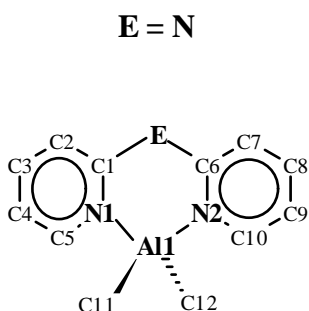
basis set for all structures. In general the structural features of the experiments could be mimicked by both methods. The vibrational assignment in the experimental spectra was feasible with the help of the BPW91 calculations. While the vibrations calculated using B3LYP have to be scaled by $k = 0.97$, the wavenumbers were in good agreement with experiment.[17] Therefore we compare the geometrical features derived from that method to the experiments.

The calculations reasonably represent the solid state experimental parameters. The ring nitrogen atoms in the amine $(2\text{-Py})_2\text{NH 1}$ are oriented *trans* with respect to the central nitrogen atom.[16] The central N1 and the three neighboring

Table 2 Selected calculated structural parameters for $\text{Py}_2\text{PH 2}$ (bond lengths [pm], angles [$^\circ$])

	BPW91		BLYP		B3LYP
	6-31+G*	6-31G*	6-31G	6-31+G*	6-31+G*
P1-H1	142.7	142.7	145.3	142.9	141.7
P1-C1	186.6	186.5	190.4	187.9	186.1
C1-N1	135.1	135.1	136.0	135.6	134.3
N1-C5	134.8	134.7	136.2	135.3	134.0
C5-C4	140.3	140.2	140.5	140.6	139.6
C4-C3	140.3	140.2	140.8	140.7	139.6
C3-C2	140.0	140.0	140.6	140.4	139.4
C2-C1	141.1	140.9	141.0	141.5	140.4
C1-P1-C6	102.6	103.3	102.5	102.7	102.6

Table 3 Selected calculated structural parameters compared to crystal structure data of $\text{Me}_2\text{Al}(2\text{-Py})_2\text{N}$ **3** (bond lengths [pm], angles [°])



	B3LYP/ 6-31+G*	BPW91/ 6-31+G*	Expt.
E-C1	134.1	134.7	134.3(2)
C1-N1	138.0	139.2	136.6(2)
N1-C5	136.4	136.8	136.6(2)
C5-C4	137.4	138.4	135.7(3)
C4-C3	141.5	141.8	139.5(3)
C3-C2	137.3	138.2	135.3(3)
C2-C1	143.2	143.6	142.3(3)
Al1-C11	198.0	198.8	195.0(2)
Al1-C12	198.0	198.8	195.0(2)
Al1-N1	195.9	197.1	191.6(2)
Al1-N2	195.9	197.0	191.4(2)
C1-E-C6	127.6	127.5	125.5(2)
N1-Al1-N2	93.7	93.6	93.5(1)

atoms are in a plane, indicating sp^2 hybridization of N1 (Figure 5).

The average central (H)N-C distance (139.4 (calc.) and 138.7(2) pm (exp.)) [16c]) is of the length of a standard $\text{N}(sp^2)\text{-C}(sp^2)$ bond distance of 140 pm. [14] In general the calculated distances in the rings are marginally longer than in the solid state crystal structure. Nevertheless it is obvious from both data that the N-C and C-C bond length do not differ, indicating full conjugation. Selected calculated geometrical parameters of $(2\text{-Py})_2\text{NH}$ **1** are compared with experimental data in Table 1.

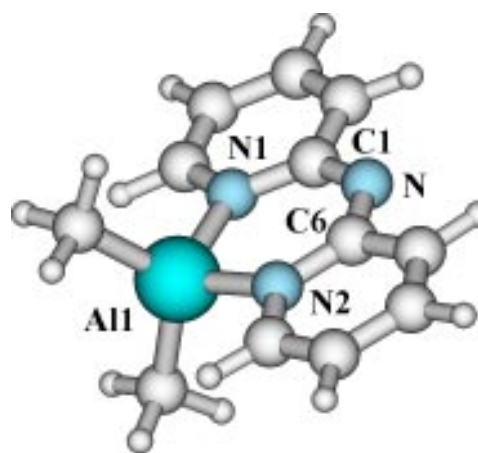


Figure 7 BPW91/6-31+G* optimized geometry of $\text{Me}_2\text{Al}(2\text{-Py})_2\text{N}$ **3**

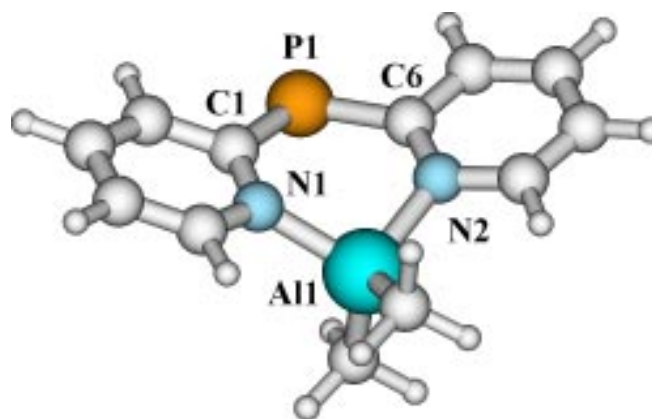


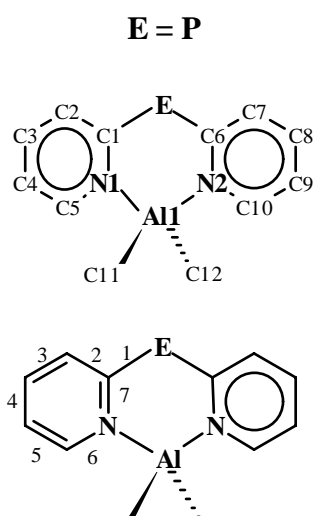
Figure 8 BPW91/6-31+G* optimized geometry of $\text{Me}_2\text{Al}(2\text{-Py})_2\text{P}$ **4**

The same is valid for the rings in the calculated di(2-pyridyl)phosphane **2**. The N-C and C-C bonds, respectively, are of the same lengths (Figure 6; Table 2)

In contrast to the central nitrogen atom in **1**, the central phosphorous atom in **2** clearly shows a pyramidal environment. The C1-P1-C6 angle of 102.6° is much more acute than the C1-N1-C6 angle in **1** (132.7°). As in **1**, the two ring nitrogen atoms are arranged in the *trans* conformation relative to the P atom. The BPW91/6-31+G* calculated P-C_{ipso} distance of 186.6 pm almost exactly matches the standard value of a P-C single bond of 185 pm. [14] Deprotonation of **1** and **2** and subsequent ring coordination to a R_2Al^+ moiety in $\text{Me}_2\text{Al}(2\text{-Py})_2\text{N}$ **3** and $\text{Me}_2\text{Al}(2\text{-Py})_2\text{P}$ **4** has a considerable impact to the structures of the related complexes in comparison to the parent amine and phosphane (Figures 7 and 8; Tables 3 and 4):

- The two ring nitrogen atoms are arranged *cisoid* with respect to the central N- and P atoms and coordinated to the aluminum atom.

Table 4 Selected calculated structural parameters compared to crystal structure data of $\text{Me}_2\text{Al}(\text{2-Py})_2\text{P}$ **4** (bond lengths [pm], angles [$^\circ$])



	B3LYP/ 6-31+G*	BPW91/ 6-31+G*	Expt.
E-C1	180.2	180.4	178.2(2)
C1-N1	137.5	138.5	136.8(2)
N1-C5	136.3	136.8	136.2(2)
C5-C4	137.6	138.5	135.8(2)
C4-C3	141.2	141.8	139.8(3)
C3-C2	137.7	138.6	136.2(3)
C2-C1	142.5	143.0	141.5(2)
Al1-C11	198.5	199.3	195.5(2)
Al1-C12	197.6	198.4	195.2(2)
Al1-N1	196.4	197.4	192.4(1)
Al1-N2	196.4	197.4	191.9(1)
C1-E-C6	106.2	106.2	106.6(7)
N1-Al1-N2	97.6	97.1	98.8(6)

- The central N-C bond is shortened by 4.4 pm and the central P-C bond by 8.2 pm, indicating partial double bond character.

- Full conjugation of the pyridyl rings is precluded and partial double bond character is found in the 3- and 5-positions.

Predominantly the last two features indicate that the resonance forms **a** and **c** in Scheme 2 contribute most to the bond description in the complexes **3** and **4**. However, while the *a priori* $4e^-$ donor capacity of the ligand can be ruled out by these findings, the question of to what extent it is a $2e^-$ donor remains open.

Raman spectroscopical results

The partial localization of the ring double bonds in **3** versus **1** and **4** versus **2** is clearly verified by Raman spectroscopical experiments. Especially the wavenumbers shifts in the $\nu(\text{C}=\text{C})$ and $\nu(\text{C}=\text{N})$ region indicate this feature.

The Raman spectrum of **3** (partially shown in Figure 9) is dominated by intense bands in the wavenumber region between 1200 and 1300 cm^{-1} . The band at 1255 cm^{-1} is assigned to the deformation vibration $\delta(\text{CH}_3)$. The two methyl groups in **3** are equivalent and give only rise to a single signal. The other bands are assigned to $\delta(\text{CN})$ at 1302 and 1290 cm^{-1} . In this region the $\delta(\text{CH})_{\text{ar}}$ are also observed and combined with the previous bands. The $\delta(\text{CNH})$ deformation for secondary amines with aromatic groups occurs between 1550 and 1650 cm^{-1} [18] and is assigned to the strong signal in **1** at 1594 cm^{-1} . Figure 9 shows several band shifts that indicate localization of double bonds in the 3- and 5- positions in the pyridyl rings. The signals at 1552 and 1486 cm^{-1} are assigned to a partial $\nu(\text{C}=\text{N})$ stretching vibration, indicating the partial C=N double bond at the bridging position (Table 5).

In general the $\nu(\text{C}=\text{N})$ and $\nu(\text{C}=\text{N})$ stretching vibrations occur at about 1630-1650 cm^{-1} and 1280-1360 cm^{-1} [18]. The $\nu(\text{Al}-\text{CH}_3)$ stretching and $\rho(\text{CH}_3)$ rocking vibrations are assigned at 672 and 578 cm^{-1} (not shown in Figure 9). The pure $\nu_s(\text{Al}-\text{CH}_3)$ stretching vibration is found at 556 cm^{-1} (calc. 557 cm^{-1}). The $\nu_s(\text{Al}-\text{N})$ and $\nu_{\text{as}}(\text{Al}-\text{N})$ stretching modes are found at 377 and 393 cm^{-1} (calc. 363 and 377 cm^{-1}). They are combined with the middle ring breathing.

The $\nu(\text{PH})$ stretching vibration of **2** occurs at 2306 cm^{-1} and disappears after the reaction with trimethyl aluminum because of to the elimination of methane. Because of the anharmonicity, the calculated wavenumbers of the $\nu(\text{CH})$ and the $\nu(\text{PH})$ stretching vibrations are shifted compared to the experimentally observed ones. As in **3**, the characteristic

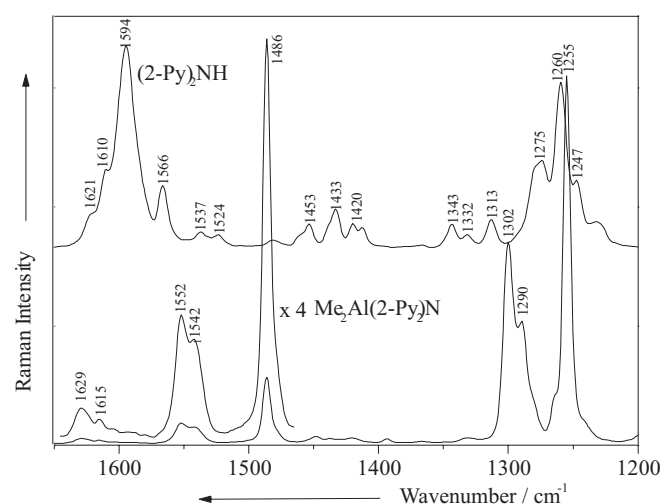
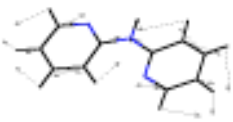
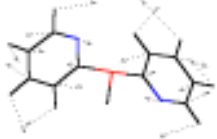
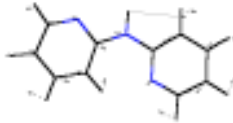
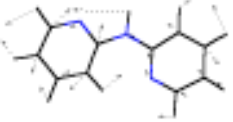
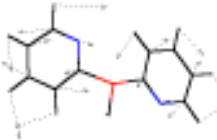
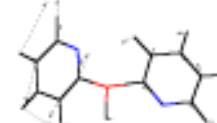
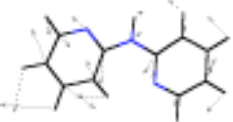
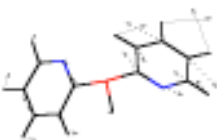
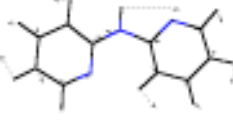


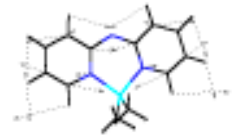

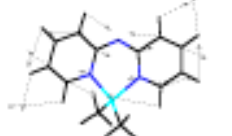

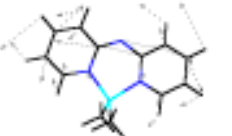
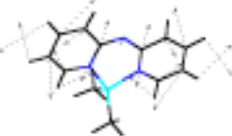
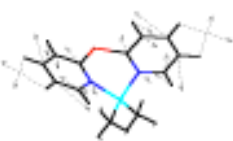
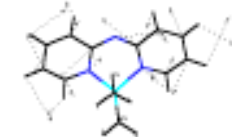
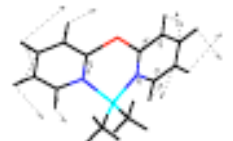
Figure 9 Part of the FT-Raman spectra of $(\text{2-Py})_2\text{NH}$ **1** and $\text{Me}_2\text{Al}(\text{2-Py})_2\text{N}$ **3**

Table 5 Calculated (BPW91/6-31+G*) $\nu(\text{C}=\text{C})$ and $\nu(\text{C}=\text{N})$ stretching vibrations in (2-Py)₂NH **1** (left column) and (2-Py)₂PH **2** (right column). Experimental values for the wavenumbers are also given in brackets for comparison

	
1610 cm ⁻¹ (1621, 1610 cm ⁻¹)	1581 cm ⁻¹ (1615 cm ⁻¹)
	
1595 cm ⁻¹ (1594 cm ⁻¹)	
	
1592 cm ⁻¹ (1582 cm ⁻¹)	1575 cm ⁻¹ (1592 cm ⁻¹)
	
	1565 cm ⁻¹ (1574 cm ⁻¹)
	
1574 cm ⁻¹ (1566 cm ⁻¹)	1564 cm ⁻¹ (1561 cm ⁻¹)
	
1524 cm ⁻¹ (1537, 1524 cm ⁻¹)	

stretching vibrations $\nu(\text{C}=\text{C})$ and $\nu(\text{C}=\text{N})$ from the pyridyl rings show a significant shift in the region between 1650 and 1500 cm⁻¹ (Table 6). Unfortunately, the $\nu(\text{PC})$ vibrational modes in **2** and **4** are combined with the pyridyl ring vibrations (1080 – 1200 cm⁻¹), so that direct comparison of their bond strength is precluded. The calculation predicts only one signal for the $\delta(\text{CH}_3)$ in the planar molecule of **3**, whereas two signals are calculated for the butterfly conformation in **4**. The difference between the two calculated signals is 11 cm⁻¹ and has been verified in the experiment. The $\nu(\text{Al}-\text{CH}_3)$

Table 6 Calculated (BPW91/6-31+G*) $\nu(\text{C}=\text{C})$ and $\nu(\text{C}=\text{N})$ stretching vibrations in Me₂Al(2-Py)₂N **3** (left column) and Me₂Al(2-Py)₂P **4** (right column). Experimental values for the wavenumbers are given in brackets for comparison

	
1631 cm ⁻¹ (1629 cm ⁻¹)	1602 cm ⁻¹ (1606 cm ⁻¹)
	
1615 cm ⁻¹ (1615 cm ⁻¹)	1598 cm ⁻¹ (1592 cm ⁻¹)
	
1556 cm ⁻¹ (1552 cm ⁻¹)	
	
1546 cm ⁻¹ (1542 cm ⁻¹)	1540 cm ⁻¹ (1535 cm ⁻¹)
	
1504 cm ⁻¹ (1486 cm ⁻¹)	1521 cm ⁻¹ (1512 cm ⁻¹)

stretching and $\rho(\text{CH}_3)$ rocking vibrations are assigned to 666 and 574 cm⁻¹, respectively. The pure $\nu(\text{Al}-\text{CH}_3)$ stretching vibration is found at 521 or 554 cm⁻¹ (cal. 554 cm⁻¹). In the region of 500-400 cm⁻¹ in the spectra several PC deformation vibrations occur. The $\nu(\text{Al}-\text{N})$ stretching modes are combined with the middle ring breathing, which is localized at 350 and 370 cm⁻¹ (calculated 335 and 338 cm⁻¹).

The calculated vibrations of **3** and **4** using BPW91/6-31+G* are in good agreement with the experiments. The difference in the first two $\nu(\text{C}=\text{C})$ modes of **3** and **4** is 14 cm⁻¹, in both experiment and theory. Comparison of the wavenumbers for these vibrations in **3** and **4** reveals a shift of 23 cm⁻¹ to higher wavenumbers in **3** relative to **4**. This shift indicates higher partial double bond localization in the 3- and 5-positions in **3**. The vibrations at 1542 in **3** and 1535 cm⁻¹ in **4** indicate stronger bonds in the 4- and 7-ring positions of **3** relative to **4**. Hence, all bonds in **3** are strength-

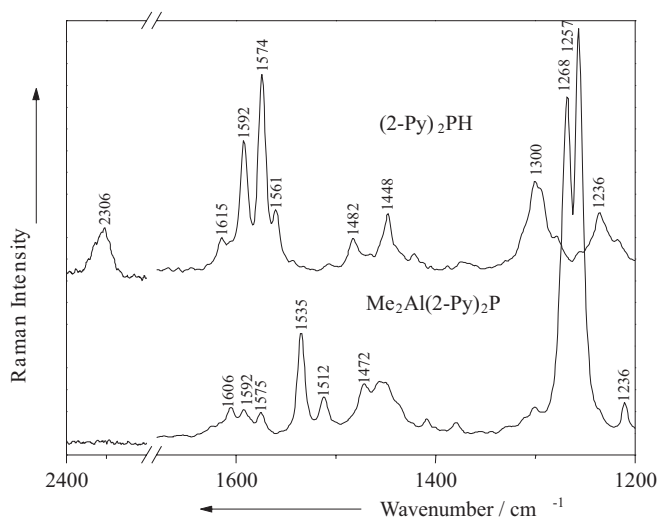


Figure 10 Part of the FT-Raman spectra of Py_2PH **2** and $\text{Me}_2\text{Al}(\text{2-Py})_2\text{P}$ **4**

ened, while partial double bond localization is emphasized in **4**. Furthermore, the vibrations at 1551 and 1486 cm^{-1} in **3** show partial $\nu(\text{N}=\text{C})$ stretching of the $\text{N}-\text{C}_{\text{ipso}}$ bond combined to the $\nu(\text{C}=\text{C})$ stretching wavenumber of the 3- and 5-positions. Comparison of the vibrations at 1486 and 1512 cm^{-1} is hindered because an $\text{E}-\text{C}_{\text{ipso}}$ contribution occurs in **3** but not in **4**. The shift of 27 cm^{-1} for the $\nu_{\text{as}}(\text{Al}-\text{N})$ and 23 cm^{-1} for the $\nu_{\text{s}}(\text{Al}-\text{N})$ stretching vibration of **3** versus **4** to higher wavenumbers indicates different Al-N bonding, possibly due to different coordination geometries in the complexes.

Furthermore, we performed electron density calculation for **3** and **4**. The two representations depicted in Figure 11 show a clear difference in the total electron density distribution. While the charge density in the amide ligand in $\text{Me}_2\text{Al}(\text{2-Py})_2\text{N}$ **3** indicates considerable electron density at the central bridging nitrogen atom (Figure 11 left), there is almost no density remaining at the central bridging phosphorus atom in $\text{Me}_2\text{Al}(\text{2-Py})_2\text{P}$ **4** (Figure 11 right). Hence, the Lewis basicity of this atom is quite low compared to the nitrogen atoms. These findings confirm the formation of metal nitrogen rather than metal phosphorous bonds even in reaction pathways, which have been recently established computationally by Budzelaar in the reaction of (2-pyridyl)phophanes with methyl lithium.[19]

Conclusion

All di(2-pyridyl) amides and -phosphides coordinate the R_2Al^+ fragment *via* both ring nitrogen atoms. This suggests that the charge density in the anions is coupled into the rings and accumulated at the ring nitrogen atoms, but the Lewis basicity of the central nitrogen atom in **5** is still high enough to coordinate a second equivalent AlEt_3 to form the Lewis acid base adduct $\text{Et}_2\text{Al}(\text{2-Py})_2\text{NAlEt}_3$ **7**. The computational tools

discussed facilitate the unambiguous assignment of the Raman ring vibrational frequencies. The shift to higher wavenumbers on going from the parent amine **1** and phosphane **2** to the metal complexes **3** and **4** indicates partial double bond localization in the ring positions **3** and **5**. This effect is more pronounced in the di(2-pyridyl)amide complexes than in the phosphide. Due to the higher electronegativity of the central nitrogen atom in **3**, **5** and **7** compared to the bridging two-coordinated phosphorus atom in **4** and **6** the di(2-pyridyl)-amide is the harder Lewis base. In the phosphides nearly all charge density couples into the rings, leaving the central phosphorus atom only attractive for soft metals. It will be the subject of further investigations to find suitable metal moieties to coordinate to the ring nitrogen atoms as well as to the central phosphorus atom in the $(\text{2-Py})_2\text{P}^-$ anion.

Experimental section

Preparation and characterization of 1-7

All manipulations are performed under an inert atmosphere of dry nitrogen gas with Schlenk techniques or in an argon drybox. All solvents were dried over Na/K alloy and distilled prior to use. NMR spectra were obtained with a Bruker AMX 400 and recorded in C_6D_6 , CDCl_3 or d_8 -toluene with SiMe_4 (^1H , ^{13}C) and H_3PO_4 (^{31}P) as standards. EI-mass spectra were measured on a Finnigan MAT 90 instrument. Elemental analyses were obtained from the Mikroanalytisches Labor des Instituts für Anorganische Chemie der Universität Würzburg.

The Raman spectra of compounds **1** - **4** were measured at room temperature at 1064 nm in NMR tubes with a Bruker spectrometer model IFS 120-HR equipped with a FT-Raman module FRA 106. **1** and **3** were measured as solids, **4** in toluene/hexane/ether solution and **2** as pure oil.

5: 4.00g (23.3 mmol) of HNPy_2 **1** in 120 mL Et_2O are reacted with the equimolar amount of Et_3Al (35.4 mL of a 15% solution in *n*-hexane, 23.3 mmol) at -78°C . The mixture is slowly allowed to warm to room temperature and stirred overnight. After removing the solvent the yellow liquid is

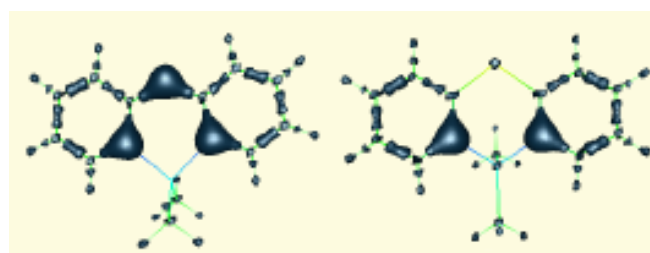


Figure 11 Total electron density of $\text{Me}_2\text{Al}(\text{2-Py})_2\text{N}$ **3** (left) and $\text{Me}_2\text{Al}(\text{2-Py})_2\text{P}$ **4** (right); ($d = 0.28 e \text{ \AA}^{-3}$). Plots were obtained by using the *gOpenMol* package (Laaksonen, L., Espoo, Finland, <http://laaksonen.csc.fi/gopenmol/gopenmol.html>)

distilled *in vacuo* affording Et₂AlNPy₂ **5** (bp. 158°C - 161°C) as a pale yellow oil. Yield: 3.87 g (65.4%); ¹H-NMR (C₆D₆, room temperature): δ 0.21 (q, 4H, ³J_{H-H} = 8.04, Al(CH₂CH₃)₂), 1.08 (t, 6H, ³J_{H-H} = 8.07, Al(CH₂CH₃)₂), 6.07 (ddd, ³J_{H-H4} = 6.42, ³J_{H-H6} = 6.41, ⁴J_{H-H3} = 1.29, 2H, H5), 6.92 (ddd, 2H, ³J_{H-H3} = 6.75, ³J_{H-H5} = 6.73, ⁴J_{H-H6} = 2.01, H4), 7.04 (d, 2H, ³J_{H-H4} = 8.79, H3), 7.32 (ddd, ³J_{H-H5} = 6.03, ⁴J_{H-H4} = 1.83, ⁵J_{H-H3} = 0.72, 2H, H6); ¹³C-NMR (C₆D₆, room temperature): δ -0.65 (s, AlCH₂CH₃), 8.87 (s, AlCH₂CH₃), 110.9 (s, C5), 125.0 (s, C4), 138.8 (s, C3), 140.5 (s, C6), 159.2 (s, C2); MS (70 eV): m/z = 170 (Py₂N, 100%), 85.5 (AlEt₂, 3.91%), 78.0 (Py, 23.9%); Anal. Calc. (found) C, 65.7 (64.3), H, 7.11 (7.20), N, 16.5 (17.1).

6: (a) 0.80g (4.25 mmol) of HPPy₂ **2** in 10 mL Et₂O are reacted with the equimolar amount of Et₃Al (4.25 mL of a 15% solution in *n*-hexane, 4.25 mmol) at -78°C. The mixture is slowly allowed to warm to room temperature and stirred overnight. Crystallization at -30° gives red crystals of Et₂AlPPy₂ **6**. Yield 0.87 g (75.3%); (b) 2.00g (7.20 mmol) of PPy₃ in 50 mL THF is reacted with an excess of lithium metal 3.00g (17.4 mmol). The deep red reaction mixture is stirred for 24 h at room temperature and filtered from non reacted lithium metal. The THF is removed under vacuum, and the precipitate is re-dissolved in 50 mL Et₂O. The solution is cooled to -40°C, and a solution of 7.2 mL of 1M (7.20 mmol) Et₂AlCl in *n*-hexane is added over a period of 1 h. The reaction solution is warmed to room temperature and stirred overnight. Lithium chloride is filtered off and 3 days storage of the clear red solution at -30°C yields dark red crystals. Yield 0.90 g (45.7%); Dp: 56°C; ¹H-NMR (C₆D₆, room temperature): δ 0.33 (q, 4H, ³J_{H-H} = 8.22, AlCH₂CH₃), 1.19 (t, 6H, ³J_{H-H} = 8.25, AlCH₂CH₃), 5.95 (ddd, 2H, ³J_{H-H4} = 7.32, ³J_{H-H6} = 6.41, ⁴J_{H-H3} = 1.32, H5), 6.36 (dddd, 2H, ³J_{H-H3} = 7.50, ³J_{H-H5} = 6.51, ⁴J_{H-H3} = 0.93, ⁴J_{H-P} = 0.91, H4), 7.29 (dddd, 2H, ³J_{H-P} = 10.1, ³J_{H-H4} = 8.43, ⁴J_{H-H5} = 1.28, ⁵J_{H-H6} = 0.86, H3), 7.51 (ddd, 2H, ³J_{H-H5} = 6.31, ⁴J_{H-H4} = 1.15, ⁵J_{H-H4} = 0.82, H6); ¹³C-NMR (C₆D₆, room temperature): δ -0.25 (s, AlCH₂CH₃), 8.03 (s, AlCH₂CH₃), 114.2 (s, C5), 128.1 (d, ²J_{C-P} = 54.3, C3), 132.3 (d, ³J_{C-P} = 18.1, C4), 141.8 (d, ³J_{C-P} = 4.01, C6), 178.0 (d, ¹J_{C-P} = 73.1, C2); ³¹P-NMR (C₆D₆, room temperature): δ = 23.7, s; MS (70 eV): m/z = 187 (Py₂P, 77.8%), 109 (PyP, 75%), 85.5 (AlEt₂, 2.95%), 78.0 (Py, 31.7%); Anal. Calc. (found) C, 61.8 (62.3), H, 6.62 (6.70), N, 10.3 (9.95).

7: (a) 2.00g (11.7 mmol) of HNPpy₂ **1** in 60 mL Et₂O are reacted with two equivalents of Et₃Al (35.4 mL of a 15% solution in *n*-hexane, 23.3 mmol) at -78 °C. The mixture is slowly allowed to warm to room temperature and stirred overnight. After reducing the solvent to 20% the yellow solution is stored at -40°C. After 24 h Et₂AlNPy₂AlEt₃ **7** was obtained as pale yellow crystals. Yield: 1.41 g (32.6%); (b) 1.00 g (3.91 mmol) of Et₂AlNPy₂ **5** are dissolved in 5 mL of hexane and the equimolar amount of Et₃Al (5.94 mL of a 15% solution in *n*-hexane, 3.91 mmol) is added at room temperature and stirred for 2 h. Crystallization at -40° gives pale yellow crystals of Et₂AlNPy₂AlEt₃ **7**. Yield: 0.59 g (59.1%); Dp: 35°C; ¹H-NMR (C₆D₆, room temperature): δ 0.20 (q, 4H, ³J_{H-H} = 8.04, Al(CH₂CH₃)₂), 0.32 (q, 6H, ³J_{H-H} = 8.05, Al(CH₂CH₃)₃), 1.10 (t, 6H, ³J_{H-H} = 8.07, Al(CH₂CH₃)₂), 1.31

Table 7 Crystallographic Data for **6** at 173(2) K and for **7** at 133(2) K

	6	7
empirical formula	C ₁₄ H ₁₈ AlN ₂ P	C ₂₀ H ₃₃ Al ₂ N ₃
formula weight	272.25	369.45
crystal size [mm]	0.3 × 0.3 × 0.4	0.4 × 0.4 × 0.5
crystal system	monoclinic	monoclinic
space group	P2 ₁ /n	C2/c
a [pm]	816.5(3)	1472.4(7)
b [pm]	1453.6(4)	1857.0(5)
c [pm]	1227.0(5)	1626.9(8)
β [°]	97.38(2)	105.32(2)
V [nm ³]	1.4442(9)	4.290(3)
Z	4	8
ρ _c [Mg m ⁻³]	1.252	1.144
μ _c [mm ⁻¹]	0.236	0.143
F(000)	576	1600
θ range [°]	3.16 – 24.96	3.32 – 22.59
no. reflns. measd.	3996	2902
no. unique reflns.	2537	2164
no. of restraints	0	0
no. of parameters	165	231
R1 [a] [<i>I</i> > 2σ(<i>I</i>)]	0.0474	0.0490
wR2 [b] (all data)	0.1290	0.1452
g ₁ ; g ₂ [c]	0.0664, 0.5145	0.1001, 4.3253
largest diff. peak and hole (e nm ⁻³)	479 and -413	381 and -464

$$[a] \quad R1 = \frac{\sum |F_o| - |F_c|}{\sum |F_o|}$$

$$[b] \quad wR2 = \sqrt{\frac{\sum w(F_o^2 - F_c^2)^2}{\sum w(F_o^2)^2}}$$

$$[c] \quad w = \frac{1}{\sigma^2(F_o^2) + (g_1 P)^2 + g_2 P}$$

$$P = \frac{(\max(F_o^2, 0) + 2F_c^2)}{3}$$

(t, 9H, ³J_{H-H} = 8.07, Al(CH₂CH₃)₃), 6.22 (ddd, 2H, ³J_{H-H4} = 6.78, ³J_{H-H6} = 6.42, ⁴J_{H-H3} = 1.25, H5), 6.69 (d, 2H, ³J_{H-H4} = 8.61, H3), 7.30 (ddd, 2H, ³J_{H-H3} = 6.99, ³J_{H-H5} = 6.71, ⁴J_{H-H6} = 1.83, H4), 7.84 (dd, 2H, ³J_{H-H5} = 5.69, ⁴J_{H-H4} = 1.63, H6); ¹³C-NMR (C₆D₆, room temperature): δ -0.28 (s, Al(CH₂CH₃)₂), 8.23 (s, Al(CH₂CH₃)₂), -0.29 (s, Al(CH₂CH₃)₃), 8.88 (s, Al(CH₂CH₃)₃), 111.7 (s, C5), 114.0 (s, C3), 136.1 (s, C4), 143.6 (s, C6), 159.5 (s, C2); MS (70 eV): m/z = 170 (Py₂N, 100%), 85.5 (AlEt₂, 3.91%), 78.0 (Py, 23.9%).

X-ray measurements of **6** and **7**

All data were collected on an Enraf-Nonius CAD4 four circle diffractometer (graphite-monochromated Mo-K α radiation, $\lambda = 71.073$ pm) equipped with a low temperature device[20] using an oil-coated shock-cooled crystal.[21] The structures were solved by direct methods (SHELXS-97[22]) and refined by full-matrix least squares methods against F² using SHELXL-97.[23] All non-hydrogen atoms were refined with anisotropic displacement parameters. All hydrogen atoms were assigned ideal positions and refined isotropically using a riding model with U_{iso} constrained to 1.2 times the U_{eq} of the parent atom. Relevant crystallographic data of **6** and **7** are given in Table 7. Crystallographic data (excluding structure factors) for the structures reported in this paper have been deposited with the Cambridge Crystallographic Data Centre as supplementary publication no. CCDC-135317 for **6** and CCDC-135318 for **7**. Copies of the data can be obtained free of charge on application to CCDC, 12 Union Road, Cambridge CB2 1EZ, UK [fax: + 44(1223)336-033; E-mail: deposit @ccdc. cam.ac.uk.

Computational details

The DFT calculations of harmonic wavenumbers were performed by utilizing fully optimized molecular geometry as the reference geometry. The DFT geometry optimization was carried out for (2-Py)₂NH **1**, (2-Py)₂PH **2**, Me₂Al(2-Py)₂N **3** and Me₂Al(2-Py)₂P **4**, with the Becke-Lee-Yang-Paar (BLYP)[24], the Becke-Perdew-Wang (BPW91)[25] gradient corrected density functional methods and the hybrid functional B3LYP[26] method. All DFT calculations were performed applying Gaussian98 [27] on DEC-Alpha, VPP-700 and VPP-300. The 6-31G, 6-31G(d), 6-31+G(d) basis sets were employed in the geometry optimization and the vibrations calculations. *Ab initio* harmonic vibrational wavenumbers (ω) are typically larger than the fundamentals (ν) observed experimentally [28]. A major source of this disagreement is the neglect of anharmonicity effects in the theoretical treatment. Errors also arise because of incomplete incorporation of electron correlation and the use of finite basis sets. Thus, for example, Hartree-Fock (HF) theory tends to overestimate bond lengths and vibrational wavenumbers because of improper dissociation behavior, a shortcoming that can be partially compensated by the explicit inclusion of electron correlation. The overestimation of *ab initio* harmonic vibrational wavenumbers is, however, found to be relatively uniform, and as a result generic wavenumber scaling factors are often applied. Good overall agreement between the scaled theoretical harmonic wavenumbers and the anharmonic experimental wavenumbers can then usually be obtained. The determination of appropriate scale factors for estimating experimental fundamental wavenumbers from theoretical harmonic wavenumbers has received considerable attention in the literature.[29]

Acknowledgement The authors thank the Deutsche Forschungsgemeinschaft (especially the SFB 347, Teilprojekte C2 and D4), the Fonds der Chemischen Industrie, Bruker axs, Karlsruhe and CHEMETALL, Frankfurt for financial support.

References

- for review see: (a) Steel, P. J. *Coord. Chem. Rev.* **1990**, 106, 227. (b) Trofimenko, S. *Prog. Inorg. Chem.* **1986**, 34, 115. (c) Constable, E. C.; Steel, P. J. *Coord. Chem. Rev.* **1989**, 93, 205. (d) Steel, P. J. *Coord. Chem. Rev.* **1990**, 106, 227. (d) Newkome, G. R. *Chem. Rev.* **1993**, 93, 2067.
- (a) Steiner, A.; Stalke, D. *J. Chem. Soc., Chem. Commun.* **1993**, 444. (b) Steiner, A.; Stalke, D. *Organometallics* **1995**, 14, 2423.
- Gornitzka, H.; Stalke, D. *Eur. J. Inorg. Chem.* **1998**, 311.
- for review see: Kottke, T.; Stalke, D. *Chem. Ber. / Rec.* **1997**, 130, 1365.
- (a) Cowley, A. H.; Jones, R. A. *Angew. Chem.* **1989**, 101, 1235; *Angew. Chem., Int. Ed. Engl.* **1989**, 28, 1208. (b) Heaton, D. E.; Jones, R. A.; Kidd, K. B.; Cowley, A. H.; Nunn, C. M. *Polyhedron* **1988**, 7, 1901. (c) Cowley, A. H.; Jones, R. A. *Polyhedron* **1994**, 13, 1149. (d) Buhro; W. E. *Polyhedron* **1994**, 13, 1131.
- (a) Howie, R. A.; Izquierdo, G.; McQuillan, G. P. *Inorg. Chim. Acta* **1983**, 72, 165. (b) Blake, A. J.; Parsons, S.; Rawson, J. M.; Winpenny, R. E. P. *Polyhedron* **1995**, 14, 1895. (c) Wang, X. M.; Sun, H. S.; Yu, X. Z. *Polyhedron*, **1996**, 15, 3543. (d) Wang, X. M.; Sun, H. S.; You, X. Z. *Polyhedron* **1996**, 15, 3543. f) Cotton, F. A.; Daniels, L. M.; Jordan IV, G. T.; Murillo, C. A. *Polyhedron* **1998**, 17, 589.
- (a) Deeming, A. J.; Smith, M. B. *J. Chem. Soc., Dalton Trans.* **1993**, 2041. (b) Engelhardt, L. M.; Gardiner, M. G.; Jones, C.; Junk, P. J.; Raston, C. L.; White, A. J. *J. Chem. Soc., Dalton Trans.* **1996**, 3053. (c) Liu, W.; Hassan, A.; Wang, S. *Organometallics* **1997**, 16, 4257. (d) Deacon, G. B.; Faulks, S. J.; Gatehouse, B. M.; Jozsa, A. J. *Inorg. Chim. Acta* **1997**, 21, L1.
- Wagaw, S.; Buchwald, S. L. *J. Org. Chem.* **1996**, 61, 7240.
- (a) Hurley, T. J.; Robinson, M. A. *Inorg. Chem.* **1968**, 7, 33. (b) Oro, L. A.; Ciriano, M. A.; Viguri, F. *Inorg. Chim. Acta* **1986**, 115, 65. (c) Aduldecha, S.; Hathaway, B. J. *J. Chem. Soc., Dalton Trans.* **1991**, 993.
- (a) Appel, R.; Knoll, F.; Ruppert, I. *Angew. Chem.* **1981**, 93, 771; *Angew. Chem., Int. Ed. Engl.* **1981**, 20, 731. (b) Appel, R.; Knoll, F. *Adv. Inorg. Chem.* **1989**, 33, 259.
- Sheldrick, G. M.; Sheldrick, W. S. *J. Chem. Soc. A* **1969**, 2279.
- Hitchcock, P. B.; Jasim, H. A.; Lappert, M. F.; Williams, H. D. *J. Chem. Soc., Chem. Commun.* **1986**, 1634.

13. Kumar, R.; de Mel, S. J.; Oliver, J. P. *Organometallics* **1989**, 8, 2488.
14. Rademacher, P. *Strukturen organischer Moleküle*; VCH: Weinheim, 1987.
15. (a) Vranka, R. G.; Amma, E. L. *J. Am. Chem. Soc.* **1967**, 89, 3121. (b) Byram, S. K.; Fawcett, J. K.; Nyburg, S. C.; O'Brian, R. J. *J. Chem. Soc., Chem. Commun.* **1970**, 16. (c) Hoffman, J. C.; Streib, W. E. *J. Chem. Soc., Chem. Commun.* **1971**, 911.
16. (a) Johnson, J. E.; Jacobson, R. A. *Acta Crystallogr., Sect. B* **1973**, 29, 1669. (b) Pyrká, G. J.; Pinkerton, A. A. *Acta Crystallogr., Sect. C* **1992**, 48, 91. (c) Schödel, H.; Näther, C.; Bock, H.; Butenschön, F. *Acta Crystallogr., Sect. B* **1996**, 52, 842.
17. Fleischer, R.; Walfort, B.; Gburek, A.; Scholz, P.; Kiefer, W.; Stalke, D. *Chem. Eur. J.* **1998**, 4, 2266.
18. (a) Dollish, F. R.; Fateley, W. G.; Bentley, F. F. *Characteristic Raman Frequencies of Organic Compounds*; Wiley & Sons: New York, 1974. (b) Lin-Vien, D.; Colthup, N. B.; Fateley, W. G.; Grasselli, J. G. *The Handbook of Infrared and Raman Characteristic Frequencies of Organic Molecules*; Academic Press: New York, 1991.
19. Budzelaar, P. H. M. *J. Org. Chem.* **1998**, 63, 1131.
20. Stalke, D. *Chem. Soc. Rev.* **1998**, 27, 171.
21. Kottke, T.; Stalke, D. *J. Appl. Crystallogr.* **1993**, 26, 615.
22. Sheldrick, G.M. *Acta Crystallogr., Sect. A* **1990**, 46, 467.
23. Sheldrick, G. M. SHELLX-97 program for crystal structure refinement; Universität Göttingen, 1997.
24. (a) Becke, A. D. *Phys. Rev. A* **1988**, 38, 3098. (b) Lee, C.; Yang, W.; Parr, R. G. *Phys. Rev. B* **1988**, 37, 785.
25. Perdew, J. P.; Wang, Y. *Phys. Rev. B* **1992**, 45, 13244.
26. Becke, A. D. *J. Chem. Phys.* **1993**, 98, 5648.
27. Gaussian98, Revision A5.; Frisch, M. J.; Trucks, G. W.; Schlegel, H. B.; Gill, P. M. W.; Johnson, B. G.; Robb, M. A.; Cheesman, J. R.; Keith, T.; Petersson, G. A.; Montgomery, J. A.; Rhaghavachari, K.; Al-Laham, M. A.; Zakrzewski, V. G.; Ortiz, J. V.; Foresman, J. B.; Ciolowski, J.; Stefanov, B. B.; Nanayakkara, A.; Challacombe, M.; Peng, C. Y.; Ayala, P. Y.; Chen, W.; Wong, M. W.; Andres, J. L.; Replogle, E. S.; Gomberts, R.; Martin, R. L.; Fox, D. J.; Binkley, J. S.; Defrees, D. J.; Baker, J.; Stewart, J. P.; Head-Gordon, M.; Gonzalez, C.; Pople, J. A. Gaussian, Inc., Pittsburg PA, 1998.
28. Hehre, W. J.; Radom, L.; Schleyer, P. v. R.; Pople, J. A. *Ab Initio Molecular Orbital Theory*; Wiley & Sons: New York, 1986.
29. Scott, A. P.; Radom, L. *J. Phys. Chem.* **1996**, 100, 16502.